New Phytologist

Research

Geometric cues forecast the switch from two- to three-dimensional growth in *Physcomitrella patens*

Han Tang[1,2], Kilian Duijts[2], Magdalena Bezanilla[3], Ben Scheres[1], Joop E. M. Vermeer[4] and Viola Willemsen[1]

[1]Laboratory of Plant Developmental Biology, Wageningen University & Research, 6708 PB, Wageningen, the Netherlands; [2]Laboratory of Cell Biology, Wageningen University & Research, 6708 PE, Wageningen, the Netherlands; [3]Biological Sciences Department, Dartmouth College, Hanover, NH 03755, USA; [4]Laboratory of Cell and Molecular Biology, Institute of Biology, University of Neuchâtel, 2000 Neuchâtel, Switzerland

Author for correspondence:
Viola Willemsen
Tel: +31 317 481 182
Email: viola.willemsen@wur.nl

Received: *28 May 2019*
Accepted: *12 October 2019*

New Phytologist (2019)
doi: 10.1111/nph.16276

Key words: 2D-to-3D development, asymmetric cell division, cell fate switch, geometric cues, *Physcomitrella patens*.

Summary

- During land colonization, plants acquired a range of body plan adaptations, of which the innovation of three-dimensional (3D) tissues increased organismal complexity and reproductivity. In the moss, *Physcomitrella patens*, a 3D leafy gametophore originates from filamentous cells that grow in a two-dimensional (2D) plane through a series of asymmetric cell divisions. Asymmetric cell divisions that coincide with different cell division planes and growth directions enable the developmental switch from 2D to 3D, but insights into the underlying mechanisms coordinating this switch are still incomplete.
- Using 2D and 3D imaging and image segmentation, we characterized two geometric cues, the width of the initial cell and the angle of the transition division plane, which sufficiently distinguished a gametophore initial cell from a branch initial cell. These identified cues were further confirmed in gametophore formation mutants.
- The identification of a fluorescent marker allowed us to successfully predict the gametophore initial cell with >90% accuracy before morphological changes, supporting our hypothesis that, before the transition division, parental cells of the gametophore initials possess different properties from those of the branch initials.
- Our results suggest that the cell fate decision of the initial cell is determined in the parental cell, before the transition division.

Introduction

During plant evolution, the transition to land coincided with the innovation of three-dimensional (3D) growth (Graham *et al.*, 2000; Whitewoods *et al.*, 2018), suggesting that the 'escape' from planar growth was a significant step in the colonization of land. The early land plant lineage developed shooting systems that allow them to grow upwards and to evolve radially positioned organs, which increase the degree of productivity and complexity. These shooting systems depended on a novel stem cell function that was capable of rotating cell division planes (Harrison *et al.*, 2009). Conversely, the algal sister groups of land plants generally grow as two-dimensional (2D) filaments.

In the moss, *Physcomitrella patens*, the main growing tissue is composed of 2D filamentous protonemata cells, from which a 3D gametophore tissue can be formed through a series of asymmetric cell divisions. In the protonema stage, cells grow by tip growth along with the emergence of branches. The transition from 2D to 3D growth is initiated from one asymmetric cell division that generates a new gametophore initial cell from its parental filament at the branching site (Harrison *et al.*, 2009), hereafter referred to as the 'transition division' (Fig. 1a). The branch initial cell elongates by tip cell growth and divides in a horizontal plane, whereas the gametophore initial cell swells and executes a first oblique division. Three-dimensional growth commences after this oblique division, which gives rise to one apical stem cell and one basal cell. Two following divisions that occur roughly perpendicular to the oblique division plane result in a tetrahedral apical stem cell, from which a gametophore is established (Whitewoods *et al.*, 2018). Cell swelling and the oblique division are therefore two visible morphological markers of the 3D growth initiation. Approximately 5% of protonema side branches develop into gametophore initial cells (Cove & Knight, 1993; Kofuji & Hasebe, 2014). The coordination of division plane orientations and gametophore cell identity thus plays a vital role during the 2D-to-3D transition. A central question is this: At what stage is the cell fate of gametophore initial instead of side branch initial determined?

Two plant hormones, auxin and cytokinin, induce the transition from 2D filament to 3D gametophore development (Ashton *et al.*, 1979; Cove *et al.*, 2006). Exogenous application of cytokinin increases the number of emerging early gametophores,

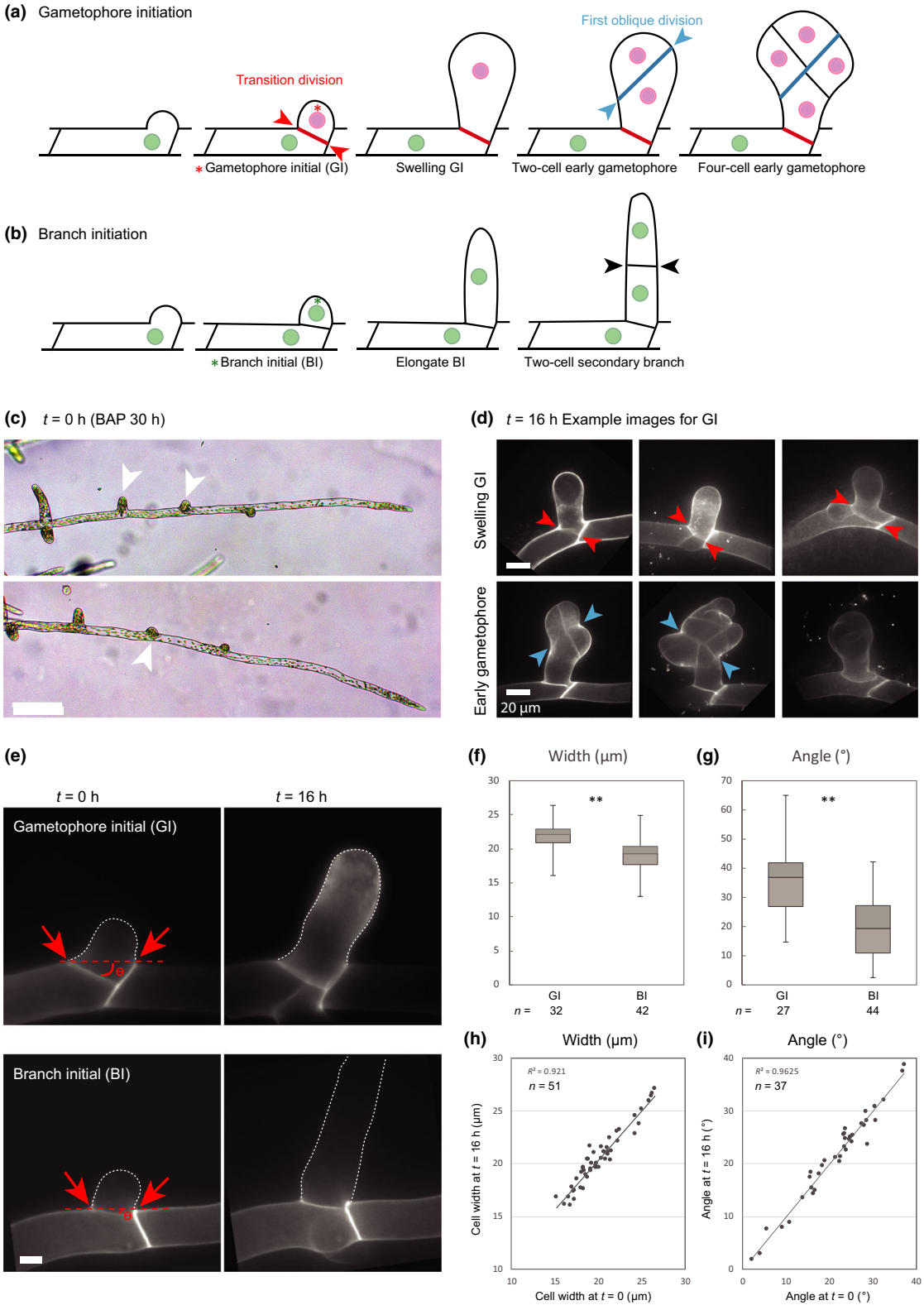

while auxin stimulates the formation of early gametophore in a cytokinin-dependent manner (Ashton *et al.*, 1979; Prigge & Bezanilla, 2010; Aoyama *et al.*, 2012). Homologs of master regulators of stem cell specification in angiosperms, APETALA2-type transcription factors, *PpAPBs*, are indispensable for gametophore formation (Aoyama *et al.*, 2012). As the orthologous genes to *PpAPBs* in Arabidopsis are essential in stem cell niche formation, cell proliferation and embryogenesis (Elliott *et al.*, 1996;

Fig. 1 Before swelling, gametophore initial cells are geometrically distinct from branch initial cells. (a) Schematic representation of gametophore initiation. The transition division that cleaves a gametophore initial cell and its parental cell is depicted by a red line and red arrowheads; the first oblique division in a swelling gametophore initial cell is shown by a blue line and blue arrowheads. Nuclei of parental cells are indicated in green and for different gametophore stages in pink. The early gametophore is defined from two cells until the stage with visible leafy structures. (b) Schematic representation of branch initiation. The orientation of cell division is perpendicular to cell growth axis as indicated by black arrowheads. Nuclei of parental cells and secondary branch filaments are indicated in green. (c) Wild-type *Physcomitrella patens* tissue was cultured in an imaging dish for 6 d, and treated with 6-benzylaminopurine (BAP) for 30 h to induce gametophore formation. Potential gametophore initial cells were indicated by white arrowheads. Bar, 0.1 mm. (d) Example images of swelling gametophore initials and early gametophores with multiple divisions. The images were captured at $t = 16$ h, when cells were treated with BAP for a total of 46 h. The transition division is depicted by red arrowheads, and the first oblique divisions are depicted by blue arrowheads. Bars, 20 μm. (e) Representative images of gametophore and branch initial cells and their future fate after 16 h. The initial cells were stained with propidium iodide and observed at $t = 0$ by spinning disk microscopy; the same target cells were revisited after 16 h to confirm their cell fates by cell swelling or elongation. The projected images were reoriented such that the parental cell membrane was horizontal. The red arrowheads indicate cell length measured; the angle (θ) was measured between the horizontal axis depicted by the red dashed lines and the division plane. Bar, 10 μm. (f, g) Measurement of the cell width and the angle of the division plane as indicated in (a). The number of gametophores and branches collected from three independent experiments was indicated ($n = 3$). The horizontal line in the box denotes the median value of all collected individual cells. **, $P < 0.01$ (significant difference between three means of gametophore and branch datasets using Student's two-tailed *t*-tests). Error bars are SDs. (h, i) Correlation coefficient of cell width and the angle of division plane between time $t = 0$ h and $t = 16$ h.

Boutilier *et al.*, 2002; Aida *et al.*, 2004; Galinha *et al.*, 2007), it has been proposed that *PpAPBs* specify gametophore initial cell identity (Aoyama *et al.*, 2012). Persistent APB activity marks the gametophore initial cell, whereas *APB* expression rapidly diminishes in branch protonemal cells. Additionally, mutations in the *NO GAMETOPHORE 1-REFERENCE (Ppnog1-R)* gene causes defects in early gametophore formation (Moody *et al.*, 2018). Deletion of another gene, *DEFECTIVE KERNEL 1 (DEK1),* causes multiple early gametophore initiation events followed by aberrant gametophore development. In addition, it was recently reported that CLAVATA (CLV) signaling is also essential for gametophore initiation, orientation of the first oblique division, development of mature gametophores, and cell proliferation in the gametophore base of *Physcomitrella* (Whitewoods *et al.*, 2018). The cytoskeleton has been reported to play a key role in orienting spindle angles during swelling of the gametophore initial cell that ultimately results in the oblique division (Kosetsu *et al.*, 2017). How hormones, regulatory genes such as *PpAPBs* and *CLV*, and the cytoskeleton coordinately control asymmetric cell divisions and morphological changes remains unknown.

In the model plant Arabidopsis, multiple early embryonic cells acquire new identities with various cell shapes via a series of asymmetric cell divisions (Scheres *et al.*, 1994; Yoshida *et al.*, 2014). Computational simulation at the early embryo stage indicated that cell shape, cortical microtubules and auxin effects can be sufficient to predict the orientation of division planes (Chakrabortty *et al.*, 2018). Accumulating evidence implicates regulatory genes, the cytoskeleton and hormones in this process (Boyer & Simon, 2015; Pillitteri *et al.*, 2016), but it is still a challenge to study this process in mechanistic detail in seed plants.

Here, we used the moss *P. patens* as a system to investigate the regulation of asymmetric cell divisions. In a previous study, the identity of the gametophore fate was confirmed by the appearance of cell swelling and the oblique division (Harrison *et al.*, 2009). Until now most studies of the transitions from 2D to 3D growth in moss have focused on the oblique division during gametophore initiation, which occurs well after the transition division (Fig. 1a). Although it has been proposed that the transition from filamentous to gametophore fate occurs before the swelling and oblique division for about a decade (Harrison *et al.*, 2009), no differences between gametophore and branch initial cells before swelling and the oblique division have been reported as yet. Here, we performed 2D imaging and 3D geometric analysis to examine if a gametophore initial cell reveals detectable morphological differences from a branch initial cell within the small time window between the transition division and swelling. Our analysis reveals that a gametophore initial cell possesses significant geometric differences from a branch initial cell, sufficient to predict the gametophore fate with an accuracy of *c.* 90%. To verify the gametophore fate prediction, a fluorescent marker was introduced that predicts gametophore cell fate at the initial stage. This feature allowed us to predict the cell fate of the gametophore initial cell before notable swelling with an accuracy of *c.* 90%. The high prediction accuracy suggests that the parent cell of a gametophore initial cell possesses different properties from that of a branch initial cell and provides a new tool for mechanistic investigation of the transition from 2D to 3D growth in moss.

Materials and Methods

Plant material and growth conditions

Wild-type *P. patens* (Gransden strain) (Ashton & Cove, 1977) was used as a standard line for the observation of gametophore initiation. Moss tissues were routinely grown on BCDAT (BCD medium contains 1 mM $MgSO_4$, 10 mM KNO_3, 45 μM $FeSO_4$, 1.8 mM KH_2PO_4 [pH 6.5 adjusted with KOH], and trace element solution (0.22 μM $CuSO_4$, 0.19 μM $ZnSO_4$, 10 μM H_3BO_3, 0.10 μM Na_2MoO_4, 2 μM $MnCl_2$, 0.23 μM $CoCl_2$, 0.17 μM KI); BCDAT is BCD medium with 1 mM CaCl2, and 5 mM diammonium (+)-tartrate) plates under continuous light at 25°C as described previously (Nishiyama *et al.*, 2000). A marker line possessing the nuclear marker 2X35S::NLS4-GFP-GUS with a synthetic plasma membrane marker SNAP-TM-mCherry driven by the maize ubiquitin promoter was used for intensiometric analysis during gametophore initiation (Bezanilla *et al.*, 2003; van Gisbergen *et al.*, 2018). Imaging of early gametophore formation was induced with 1 μM 6-benzylaminopurine (BAP) treatment, besides the mock treatment described in Fig. 3 (see later). For general imaging, protonema tissue was grown on

BCD medium in glass bottom dishes (Yamada *et al.*, 2016) for 3 d under continuous white light, then moved to red light (light transmission with wavelength > 600 nm) for another 3 d. After 3 d of growth under red light the dish was moved back to white light and supplied with ½ liquid BCD medium containing 1 μM BAP. Gametophore initiation was recorded between 30 and 54 h after BAP induction. For cell fate prediction, the imaging dish was moved back to the incubator after image acquirement for recovery overnight.

Fluorescence microscopy and staining

Live cell imaging was performed on a Roper spinning disk microscope system composed of a Nikon Ti eclipse body (Nikon®, Amstelveen, the Netherlands), Yokogawa CSU-X1 spinning disc head (Yokogawa Deutschland GmbH, Ratingen, Germany) and Photometrics Evolve 512 camera. (Teledyne Photometrics, Tucson, AZ, USA) Imaging was conducted with a Nikon ×60 Plan Apo VC oil immersion objective (NA 1.40) (Nikon), using a ×1.2 post-magnification lens fitted before the camera. Green fluorescent protein (GFP) and probes were excited using 491 nm light from a Cobolt Calypso50 laser (Cobolt AB, Solna, Sweden) and emitted light was bandpass-filtered at 497–557 nm. For propidium iodide (PI) staining and mCherry 561 nm excitation, a Cobolt Jive50 laser light was used in combination with bandpass filtering at 570–620 nm. During image digitization, a camera electron multiplication gain of 300 was employed and typical exposures were 200 ms for both GFP and mCherry probes. PI was dissolved in dH_2O at a final concentration of 10 μg ml^{-1} and added to cells just before imaging. For cell fate prediction, the memory function was used to track back positions when moving the dish back after recovery. For computational geometry analysis, cell outlines were stained and fixed with SCRI Renaissance 2200 solution (0.1% (v/v) SR2200, 1% (v/v) dimethyl sulfoxide, 0.05% (w/v) Triton-X 100, 5% (w/v) glycerol, 3.75% (w/v) paraformaldehyde in PBS buffer (pH 7.4)) (Kerstens *et al.*, 2019) and recorded using a laser scanning confocal microscope (Zeiss LSM510) with a ×40 magnification lens at 0.4 μm z-stack intervals using 405 nm excitation and detection at 450–560 nm.

Cell segmentation and volume extraction

Segmentation and volume extractions were carried out using the MorphoGraphX software (http://www.MorphoGraphX.org) designed for analysis of 3D images (de Reuille *et al.*, 2015). Acquired images of early gametophores were directly imported without modification and smoothed by 3D Gaussian filter blur function. The autoseeded watershed function was used to segment cells. After trimming unwanted tissues and correcting segments by deletion or merge functions, the marching cube algorithm with a cube size of 1 μm was used to create a 3D mesh and extract geometric information (Kerstens *et al.*, 2019). For cell width and angle measurement of the segmented initial cells, the segmented mesh was first rotated to orient the parental cell in a horizontal orientation. Images were then imported in Fiji (Schindelin *et al.*, 2012) and cell width and angle were measured using the Fiji line- and angle-drawing functions.

Cell fate prediction analysis

After PI staining, raw images were acquired in about 50 z-stacks with 0.5 μm intervals and projected by the maximum intensity in Fiji. All images were then reoriented such that the filamentous parental cell was horizontal. The width of the initial cell was measured by manual usage of the line-drawing tool in which the line was drawn along the horizontal parental membrane that connects the neck of protruding initial cells. The angle of the cell division plane that separates an initial cell and its parental cell was measured in relation to the horizontal line along with parental cell using the angle tool in Fiji. The samples with unclear division plane were discarded from the dataset to avoid miscalculation.

Statistical analysis

For statistical analysis of geometric properties, two different statistical tests were used: two-tailed Student's *t*-tests and Mann–Whitney *U*-test. The tests used are indicated in the figure legends. The selected method depends on the distribution of each dataset. For cell fate prediction analysis, binomial tests were carried out in Excel under the assumptions that each initial cell is independent of the others and that the probability of each initial cell becoming a gametophore or a branch is $P = 0.5$. Gametophore, branch and total (gametophore plus branch) cells obtained from three independent experiments were collectively analyzed, as shown in Fig. 4 (see later). Additionally, every gametophore, branch and total dataset of the three experiments was also tested separately. Only one gametophore and one branch dataset did not reveal statistical significance, but all other seven tested samples passed the binomial test with P ranging from 0.018 to 1.04308E–07.

Results

Geometric cues that predict cell fate are visible before transition division

To identify differences between gametophore and branch initial cells before visible swelling, we observed early initial cells right after the transition division (Fig. 1a). These initial cells were imaged in the presence of the cell outline staining dye PI, and their ultimate cell fates were examined after overnight recovery in the incubator and tracked by premarked positions in the microscope (Fig. 1c,d). Cell fates were identified by either cell swelling or the oblique division for gametophore initials or tip cell elongation with perpendicular division for branch initials (Fig. 1a,b,d, e). To investigate whether these observed swollen cells ultimately developed into early gametophores or whether they arrested or reversed back to filaments, we tracked swollen initial cells and confirmed their outgrowth into early gametophores with multiple divisions (Supporting Information Fig. S1a). We considered a gametophore after the oblique division but before any leafy structure can be seen as an early gametophore (Fig. 1a). Around 90–

95% of swollen gametophore initial cells continually developed into early gametophores with apparent divisions and morphological changes under two growth conditions used in this study (Fig. S1b; Video S1).

Cell fates of gametophore initial cells were confirmed after 16 h, which showed that 25% of the cells displayed characteristic swelling and 75% revealed the oblique division, whereas none of them exhibited filamentous features ($n = 32$). The width of analyzed initial cells and the division plane angle of the transition division often revealed different patterns between gametophore and branch initials. Gametophore initial cells have a wider cell width and a larger division plane angle compared with branch initial cells (Fig. 1f,g). We quantified these two parameters and found that gametophore initials have, on average, a cell width of 21.9 μm (SD = 0.45, $n = 32$) and a division angle of 34.6° (SD = 5.0, $n = 27$), the latter ranging from 15° to 65° in our observations, while branch initials revealed an average cell width of 19.7 μm, (SD = 0.59, $n = 42$) and an average division angle of 17.7° (SD = 1.24, $n = 44$) (Fig. 1f,g). Taken together, gametophore and branch initial cells differ significantly with respect to cell width and division angle.

To examine if cell width and division angle change during growth, we measured and compared these two parameters in all initial cells, including gametophore and branch initials, and their descendants by tracking the same cell after overnight recovery. We found that once the initial cell emerged from its parental cell, the cell width and the division angle were almost fixed. We observed an average cell width of 20.2 μm at the early stage and 20.6 μm ($n = 51$) after growing overnight. The division angles also did not change once the division was completed, as we observed an average division angle of 21.49° before and 21.51° ($n = 37$) after overnight growth (Fig. 1h,i), demonstrating that gametophore initials and branch initials are geometrically distinct before visible swelling.

Gametophore and branch initial cells exhibit differences in 3D geometry

Using 2D imaging, we identified two geometric cues that differ in initial cells that were fated to become either early gametophore or branch. To confirm that these subtle differences were not an artifact caused by image orientation, we analyzed image stacks of initial cells with MorphoGraphX to perform segmentation and volumetric analysis. The future fate confirmation of targeted initial cells was carried out as described earlier, which showed that after 16 h, 24% of gametophore initial cells were swollen and 76% of cells presented the oblique division, but none of them exhibited filamentous features ($n = 17$). The 3D-reconstructed shape information of initial cells can be viewed from any angle, which allowed us to visualize and measure the cell width and division angle very precisely (Fig. 2a,b). Measurements acquired from 3D-segmented images confirmed the 2D data, and they consistently showed that the base of gametophore initial cells had an average cell width of 22.7 μm (SD = 1.69, $n = 16$) and an average division angle of 31.4° (SD = 8.46, $n = 15$), while branch initial cells had an average cell width of 19.9 μm (SD = 2.23, $n = 20$) and an average division angle of 19.8° (SD = 6.65, $n = 16$) (Fig. 2c,d).

To examine whether initial cells fated to become gametophores or branches exhibited differences in cell volume or the area of the division plane connecting to the parental cell, we obtained volumetric information and quantified the interface area from the 3D analysis. To avoid variation in volume owing to cell length of chosen cells, all the images of initial cells were taken 30 h after BAP induction, which was used to synchronize gametophore induction. Second, only initial cells with longitudinal lengths between 15 and 30 μm were chosen. No visible differences in cell length between chosen initial cells of early gametophores and branches were detected as shown in Fig. S2, indicating that the comparisons of the cell volumes were unbiased between gametophore and branch initial cells. Although the cell volumes of gametophore initials were, on average, 4697.2 μm^3 ($n = 17$) and those of branch initials were 4159.4 μm^3 ($n = 21$) and did not show a significant difference, the average size of the interface area in branch initials was about 211.3 μm^2, which is significantly smaller than the average of 259.4 μm^2 observed in gametophore initial cells ($n = 17/21$ for gametophore/branch, $P = 0.02$, two-tailed t-test) (Fig. 2e,f). The larger size of the interface area in gametophore initial cells probably results from the aforementioned wider cell width and greater division angle.

Geometric cues in gametophore initial cells are independent of exogenously supplied cytokinin and consistent in gametophore mutants

Under standard growth conditions it is challenging to investigate fate transitions as only *c.* 5% of emerging branching cells ultimately commit to gametophore fate. Therefore, similar to other studies focused on gametophore development (Ashton *et al.*, 1979; Aoyama *et al.*, 2012; Moody *et al.*, 2018), we supplemented the liquid medium with exogenous cytokinin, BAP, to induce gametophore initiation. To investigate whether the observed differences in cell width and division plane were influenced by exogenous cytokinin treatment, we compared the width and angle of the division plane in the absence and presence of the synthetic cytokinin BAP (Fig. 3a). We observed the same geometric patterns in terms of width and angle in gametophore and branch initial cells (Fig. 3b,c), suggesting that the differences are not a result of additional cytokinin supply.

Next, we asked whether the geometric cues predicting cell fate persist in mutants that possess gametophore development phenotypes. In Δ*dek1* and *Ppnog1-R* mutants, gametophore initiation is induced and repressed, respectively (Perroud *et al.*, 2014; Moody *et al.*, 2018). To inhibit branching and therefore synchronize gametophore induction, plant tissues were cultured under unilateral red light for 2 wk, where the Δ*dek1* mutant showed a growth phenotype with bulbous filamentous cells (Fig. 3d); under the white light condition, the Δ*dek1* mutant exhibited filamentous cell growth that was undistinguishable from the wild-type (Perroud *et al.*, 2014). Although the growth of protonema cells in the Δ*dek1* mutant is affected by red-light illumination, induction of gametophore formation by BAP treatment is comparable to the

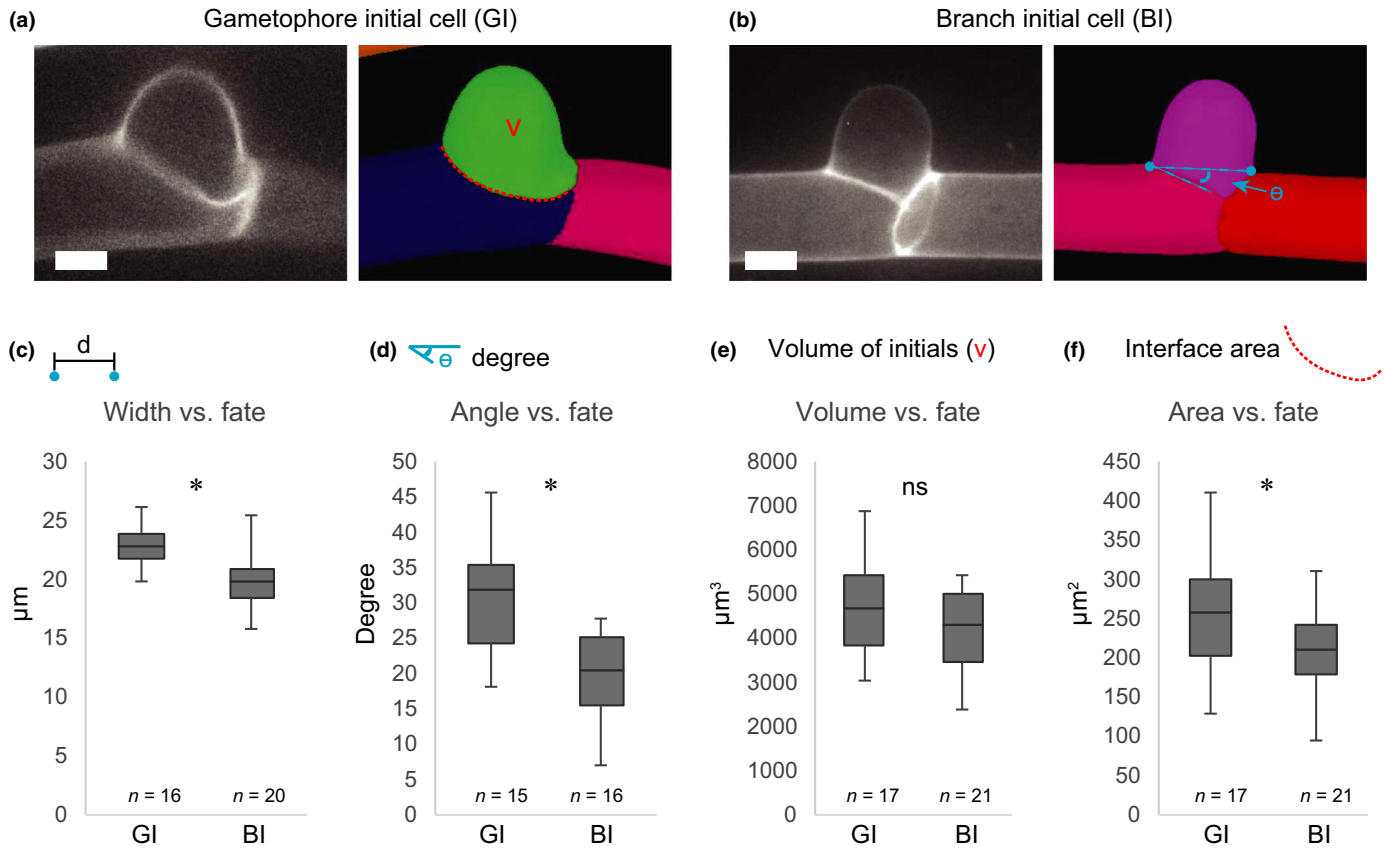

Fig. 2 Gametophore and branch initial cells exhibit differences in three-dimensional geometry. (a, b) Representative images of gametophore (a) and branch (b) initial cells and corresponding segmented images obtained from MorphoGraphX. Initial cells of wild-type *Physcomitrella patens* were stained with propidium iodide and observed by spinning disk microscopy. Blue dots in (b) indicate the length that was measured; the angle (θ) was measured between the horizontal axis and the division plane as depicted by blue dashed lines. Bars, 10 µm. The red 'v' in (a) stands for volume indication in (e); the red dotted line in (a) demonstrates the interface area for the indication in (f). (c–f) Geometric analysis of gametophore and branch initial cells. Cell fates were verified by revisiting the same cell after 16 h and confirmed by cell swelling for the gametophore or elongation for the branch (error bars are SDs): (c) cell width between the protruding site of initial cells; (d) orientation angle of division plane; (e) volume measurement of initial cells; (f) size of interface area. The number of gametophore and branch initials collected from three independent experiments is indicated. The horizontal line in the box denotes the median value of all collected individual cells. Significant differences between three means of gametophore and branch datasets (Student's two-tailed *t*-tests): *, $P < 0.05$; BI, branch initial cells; GI, gametophore initial cells; ns, not significant.

wild-type. Conversely, induction of gametophores failed in the *Ppnog1-R* mutant, in which > 99% of emerging initial cells developed to branch cells instead (Fig. 3d; in the figure the arrowhead is an early gametophore, and the arrow is a branch). To test whether the differences in the width and division angle between gametophore and branch initial cells can be observed in these two mutants, we measured the width and angle of the division plane in all developing cells after 40 h of BAP treatment.

The measurement of all emerging initial cells in Δ*dek1* mutants, in which > 90% initial cells developed into early gametophore, presented an average cell width/division angle of 24.2 µm/23.0° ($n = 47$ for width; $n = 44$ for angle) compared with 23.7 µm/25.4° in the wild-type ($n = 46$ for width; $n = 34$ for angle), showing that the mutant and wild-type had similar cell widths and angles. By contrast, the *Ppnog1-R* mutant exhibited similar patterns to wild-type branch initial cells with an average cell width of 20.3 µm ($n = 50$) and an average division angle of 16.2° ($n = 38$) (Fig. 3e–g). To exclude the possibility that the cell shape of filamentous cells causes a wider cell width or a larger divisional angle in Δ*dek1* mutants, the cell width and division angle were measured in the presence of unidirectional red light, but in the absence of BAP. Initial cells of Δ*dek1* mutants developed into branches that were indistinguishable from wild-type branches in terms of cell width and division angle, with average cell widths of 17.4 and 20.1 µm, and division angles of 13.8 and 16.5° in wild-type and Δ*dek1* mutants, respectively ($n = 17$ for wild-type; $n = 12$ for Δ*dek1*), without any statistical significance (Fig. S3). These results indicate that the geometric parameters measured in Δ*dek1* mutants in the presence of BAP were a result of the formation of gametophore initials.

The gametophore or branching cell fate can be robustly predicted using geometric cues

We identified two geometric cues, the cell width and the division angle, that differed between gametophore and branch initial cells. To test if these two parameters are good indicators to accurately predict the cell fate of emerging initial cells, the same imaging

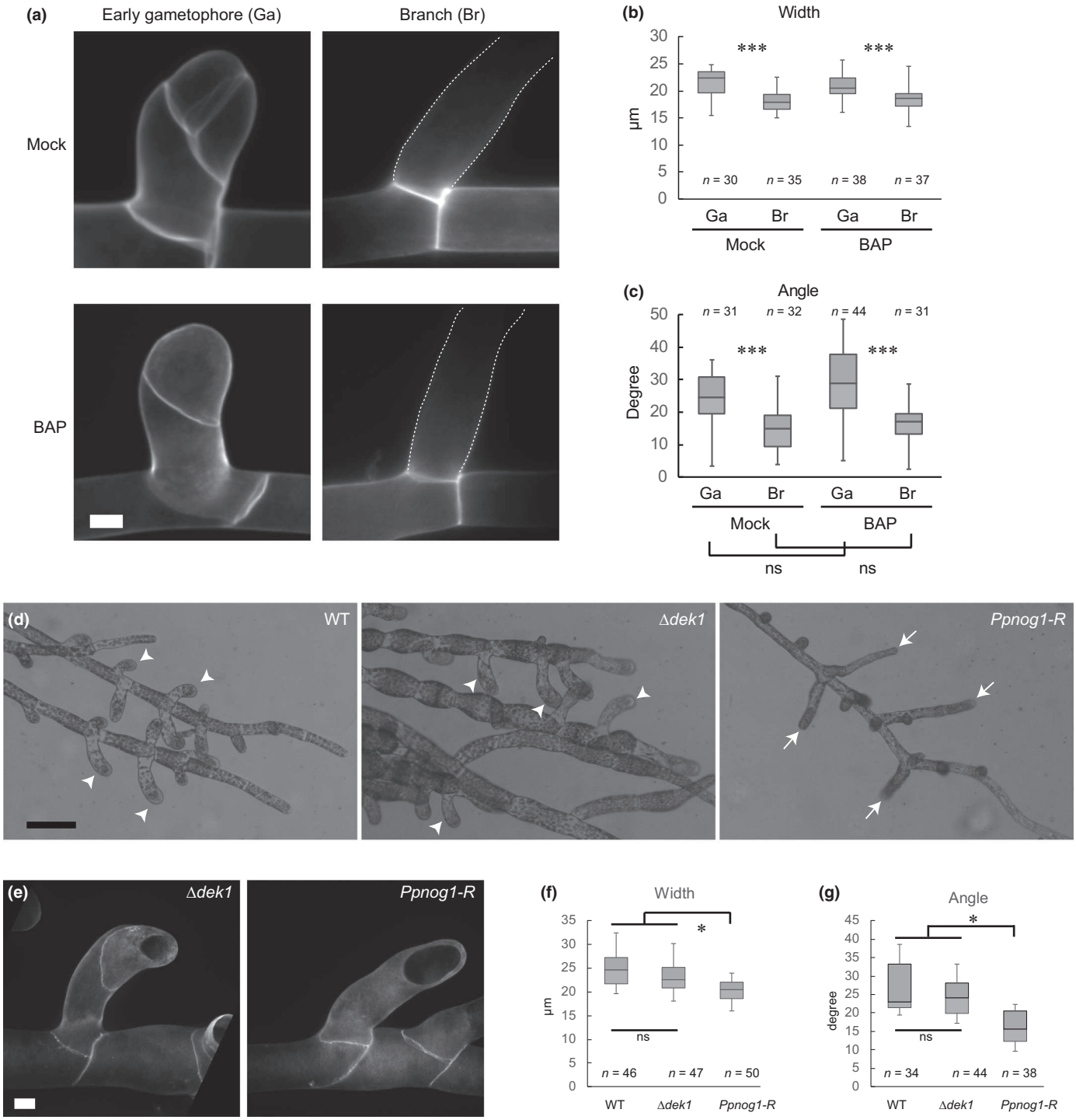

Fig. 3 Geometric cues in gametophore initials are independent of exogenously supplied cytokinin and consistent in gametophore mutants. (a) Representative images of early gametophore and branch in presence and absence of 6-benzylaminopurine (BAP) treatment as indicated. Wild-type *Physcomitrella patens* was used. The early gametophores and branches were stained with propidium iodide and imaged by spinning disk confocal microscopy. Cell outlines of branches are marked by white dotted lines. Bar, 10 µm. (b, c) measurement of the cell width and the angle of the divisional plane. The number of gametophores and branches collected from three independent experiments is indicated: ***, $P < 0.001$ (significant difference with Mann–Whitney *U*-test). Error bars are SDs. The dataset of gametophore and branch initials obtained with BAP treatment was compared with the same initial cell type without BAP treatment, which revealed no significant differences in either gametophore or branch initials. (d) Overview of gametophore induction in wild-type (WT), Δ*dek1* and *Ppnog1-R*. Plants were cultured under unilateral red light for 2 wk, followed by BAP treatment with continuous white light illumination for 40 h. Early gametophores were induced in WT and Δ*dek1* (arrowheads), but *Ppnog1-R* only formed branches under the same growth condition (arrows). Bar, 1 mm. (e) Examples of early gametophore and branch cells in Δ*dek1* and *Ppnog1-R* were stained with SCRI Renaissance 2200 and imaged by confocal microscopy. Bar, 10 µm. (f, g) Measurement of the cell width and the angle of the divisional plane. Significant differences between three means of gametophore and branch datasets: *, $P < 0.05$; ns, not significant (Student's two-tailed *t*-tests). Error bars are SDs.

tracking strategy was used with additional criteria. Based on our previous results, we set the threshold to predict a gametophore initial cell to 20 μm cell width, and 30° for the division plane angle (Fig. 1f,g). Once a candidate initial cell reached the threshold for either cell width or divisional angle, it was predicted to become a gametophore initial. The predicted result was then compared with the confirmed cell fate in order to evaluate the prediction accuracy. After 16 h, cell fates of gametophore initial cells were confirmed by either swelling (26%) or the oblique division (74%, $n = 39$). The prediction accuracy was the success rate of cells with the correct prediction, which was calculated by dividing the number of cells with confirmed cell fate by their predicted cell fate. Our prediction accuracy of around 90% ($n = 39$ for gametophores; $n = 24$ for branches) with statistical significance reinforced that gametophore initial cells exhibit geometric differences compared to branch initial cells, and that these cues are sufficient to distinguish their future cell fate at the initial stage and can be used as an early predictive tool (Fig. 4). Moreover, we propose that the observed differences in divisional planes are controlled in the parental cell, suggesting that before the transition division, and thus before the swelling, the cell fate of the gametophore initial cell is already determined.

Identification of a fluorescent marker that predicts the cell fate of the emerging initial cell

To verify that the cell fate of an initial cell is predictable at an early stage of initiation, we used an alternative strategy. We used a reporter line that carries a nuclear-localized GFP-β-glucuronidase (GFP-GUS) reporter driven by a 2X35S promoter with a synthetic plasma membrane marker (SNAP-TM-mCherry) driven by maize ubiquitin promoter (hereafter referred to as NLS4-GFP-GUS). We found that the GFP intensity was dramatically decreased in gametophore tissues at an early stage. Reduction of the nuclear GFP was already recognizable in gametophore initial cells at the swelling or two-cell stage in comparison to persistently bright signal in branch filaments (Fig. 5a). We performed time-lapse imaging to record the reduction of nuclear GFP, which showed that the GFP intensity remained high in initial cells right after the transition division, while the signal gradually decreased along with the growth and swelling of a gametophore initial cell (Video S2).

To test the predictive potential of the NLS4-GFP-GUS marker line, we first quantified the differences of GFP intensity in both gametophore and branch initial cells, because the GFP intensity on parental filaments and branch initials located on different focal planes (as shown in Fig. 5a) may result in inaccurate quantification. To overcome this, the median plane of the nucleus, recognized by the unstained area of the nucleolus, was imaged as a standard focal plane in both parental cells and initial cells. The ratio of the GFP intensity in a gametophore initial cell relative to its own parental cell was *c.* 20% ($n = 28$ for pairs of gametophore initials and parental cells) with an average intensity in gametophore initials of 347 arbitrary units (AU) and in their parental cells of 2003 AU (Fig. S4), whereas branch initials remained at *c.* 80% relative to their parental cells with an average intensity in branch initials of 1798 AU and in their parental cells of 2294 AU ($n = 27$ for pairs of branch initials and parental cells; Fig. S4). As the decrease in GFP intensity is obvious before swelling of a gametophore initial, we were able to successfully predict cell fate up to 90% (Fig. 5b,c), confirming the gametophore cell fate by cell swelling (39%) or oblique division (61%, $n = 28$). This result is consistent with previous results predicted by cell width and division angle.

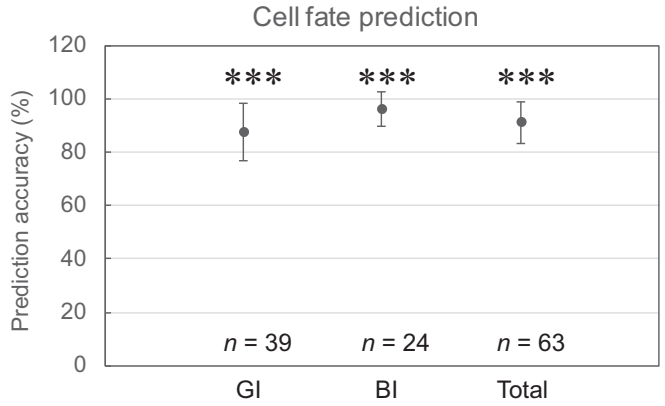

Fig. 4 Geometric cues forecast the fates of emerging initial cells. Based on the criteria in width > 20 μm and divisional angle > 30°, fates of initial cells of wild-type *Physcomitrella patens* were predicted. If the initial cell passes one of the criteria, the cell was predicted to become a gametophore. The prediction accuracy was calculated as the ratio between predicted and verified cell fates for gametophore, branch and all observed samples (total). The prediction assay was performed in three biological replicates with a total indicated number of examined cells. ***, $P < 0.001$ (significant difference using exact binomial test). BI, branch initial cells; GI, gametophore initial cells. Error bars are SDs.

Discussion

Here, we used for the first time the MorphoGraphX software for 3D image processing to accurately quantify the geometric differences between gametophore and branch initials in the moss *Physcomitrella*. Upon emergence of initial cells right after the transition division, we identified two morphological features, cell width and division angle, which distinguish gametophore and branch initial cells. Additionally, we revealed that the fluorescent reporter NLS4-GFP-GUS presented a dramatically lower nuclear GFP signal in gametophore tissues than in protonema cells. Both identified geometrical cues and the fluorescent marker allowed us to accurately predict the gametophore initial cell identity before visible swelling. In sum, we presented early markers for 2D-to-3D transition, implying that the gametophore cell fate decision occurs within a specified microenvironment in the parental cell of the initial.

The transition division is executed and regulated by the parental cell, suggesting that the decision for the transition to 3D growth has been made in the parental cell before the transition division. A parental cell can be transcriptionally specified as a founder cell and/or be the source of a specific molecular microenvironment to induce the 3D growth transition. In some cases a filamentous parental cell gives rise to a second emerging initial

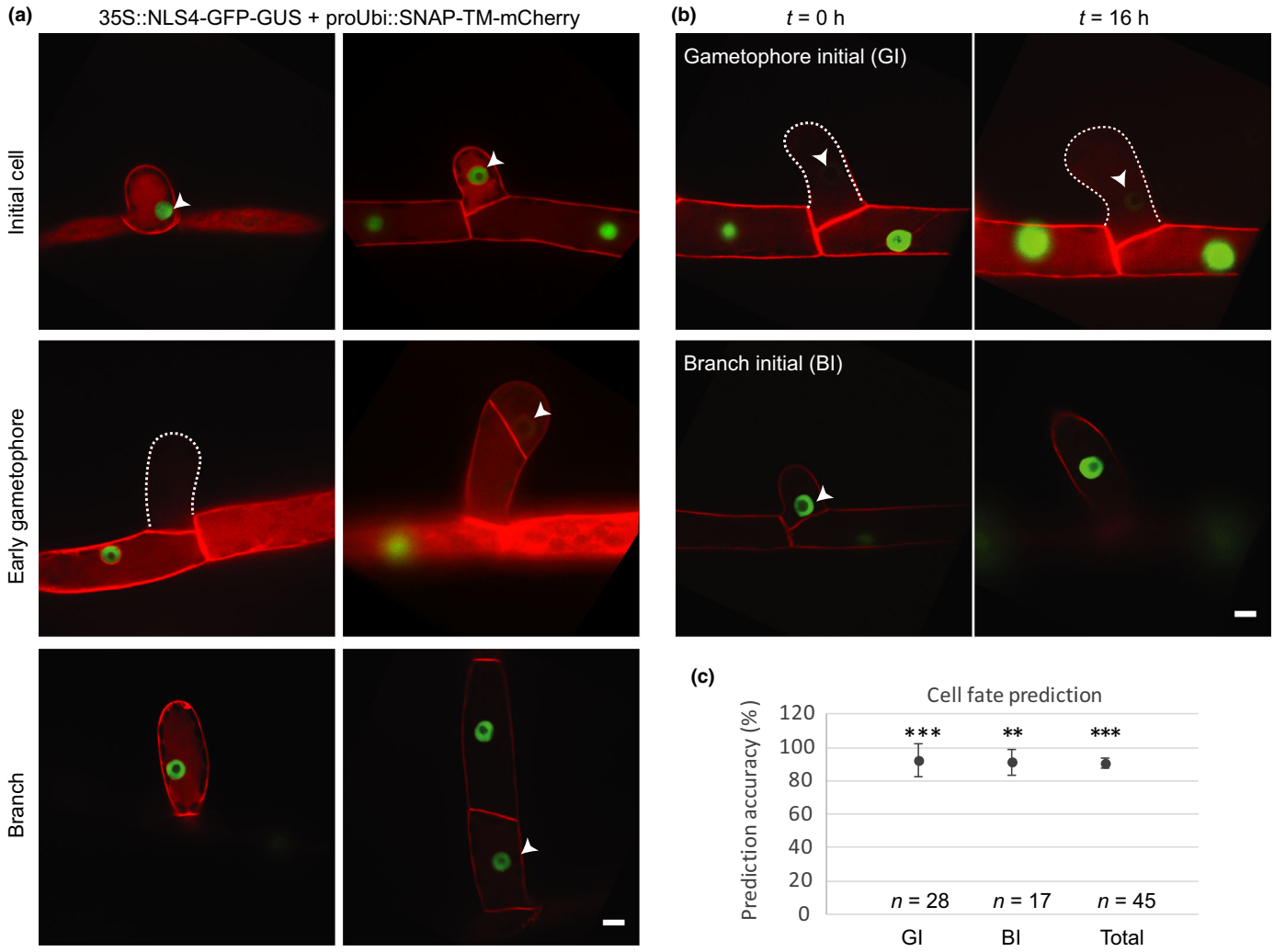

Fig. 5 Identification of a fluorescent marker to predict the cell fate of emerging initial cells. (a) Example images of undetermined initial cells, early gametophores, and branch cells with a green fluorescent-labeled nucleus (NLS4-GFP-GUS) and mCherry-labeled plasma membrane (SNAP-TM-mCherry) as indicated. Arrowheads depict the nucleus with the unstained nucleolus. *Physcomitrella patens* carrying these fluorescence markers was imaged. Bar, 10 μm. (b) Based on nuclear green fluorescent protein (GFP) intensity, the cell fated to gametophore or branch was predicted as indicated in $t = 0$ h panels. Cell fates of target initial cells were confirmed after 16 h by GFP intensity and cell morphology. (c) Prediction accuracy was calculated as the ratio between predicted and verified cell fates for gametophore, branch, and all observed samples (total). The prediction assay was performed in three biological replicates with a total indicated number of examined cells. ***, $P < 0.001$; **, $P < 0.01$ (significant difference using exact binomial test). Error bars are SDs.

cell; this requires the parental cell to re-enter the cell cycle, which is probably mediated through transcriptional control (Polyn *et al.*, 2015). Thus, it is conceivable that the specification of a parental cell giving rise to a gametophore initial takes place in parallel with the transcriptional activation of a new cell cycle. Previous reports (Harrison *et al.*, 2009) as well as our own observations (H. Tang *et al.*, unpublished) show that a gametophore and a branch can develop from the same parental cell, suggesting that the trigger for 3D transition is mediated through a transient and local specification of a parental cell. The filamentous parental cell might trigger gametophore formation via different, but not mutually exclusive, regulatory mechanisms such as transient polarity changes, cytoskeletal reorganization, and redistribution of determinants.

Our newly identified geometric markers allow early, rapid and straightforward identification of a cell transitioning into a gametophore compared with previous studies and provides a powerful tool to investigate the central question of how gametophore formation is initiated. For example, it is now possible to investigate the transition division by recognizing and isolating the gametophore initial cell and its parental cell at early stages and perform comprehensive transcriptome analysis. A transcriptomic analysis has been performed with four-cell early gametophore samples (Frank & Scanlon, 2015), and an extension of these data can provide important information on crucial initial steps of the 3D growth transition.

Acknowledgements

We thank Tijs Ketelaar and Marcel Janson in the Cell Biology group for support and discussions, Laura Moody and Viktor Demko for sharing of published material and Peter van

Gisbergen for critical reading of the manuscript. This work was supported by the Earth and Life Sciences Council (ALW) of the Netherlands Organization for Scientific Research (NWO; ALW-VIDI 864.13.008 to JEMV).

Author contributions

HT and VW planned and designed the research. HT performed the experiments. HT, KD and VW conducted data analysis. MB contributed important materials. HT, MB, BS, JEMV and VW wrote the manuscript.

ORCID

Magdalena Bezanilla https://orcid.org/0000-0001-6124-9916
Ben Scheres https://orcid.org/0000-0001-5400-9578
Han Tang https://orcid.org/0000-0001-6152-6637
Joop E. M. Vermeer https://orcid.org/0000-0001-8876-5873
Viola Willemsen https://orcid.org/0000-0002-6420-0605

References

Aida M, Beis D, Heidstra R, Willemsen V, Blilou I, Galinha C, Nussaume L, Noh Y-S, Amasino R, Scheres B. 2004. The *PLETHORA* genes mediate patterning of the Arabidopsis root stem cell niche. *Cell* **119**: 109–120.

Aoyama T, Hiwatashi Y, Shigyo M, Kofuji R, Kubo M, Ito M, Hasebe M. 2012. AP2-type transcription factors determine stem cell identity in the moss *Physcomitrella patens*. *Development* **139**: 3120–3129.

Ashton N, Cove D. 1977. The isolation and preliminary characterisation of auxotrophic and analogue resistant mutants of the moss, *Physcomitrella patens*. *Molecular and General Genetics MGG* **154**: 87–95.

Ashton NW, Grimsley NH, Cove DJ. 1979. Analysis of gametophytic development in the moss, *Physcomitrella patens*, using auxin and cytokinin resistant mutants. *Planta* **144**: 427–435.

Bezanilla M, Pan A, Quatrano RS. 2003. RNA interference in the moss *Physcomitrella patens*. *Plant Physiology* **133**: 470–474.

Boutilier K, Offringa R, Sharma VK, Kieft H, Ouellet T, Zhang L, Hattori J, Liu C-M, van Lammeren AA, Miki BL. 2002. Ectopic expression of BABY BOOM triggers a conversion from vegetative to embryonic growth. *Plant Cell* **14**: 1737–1749.

Boyer F, Simon R. 2015. Asymmetric cell divisions constructing Arabidopsis stem cell niches: the emerging role of protein phosphatases. *Plant Biology* **17**: 935–945.

Chakrabortty B, Willemsen V, de Zeeuw T, Liao C-Y, Weijers D, Mulder B, Scheres B. 2018. A plausible microtubule-based mechanism for cell division orientation in plant embryogenesis. *Current Biology* **28**: 3031–3043.e3032.

Cove D, Bezanilla M, Harries P, Quatrano R. 2006. Mosses as model systems for the study of metabolism and development. *Annual Review of Plant Biology* **57**: 497–520.

Cove DJ, Knight CD. 1993. The moss *Physcomitrella patens*, a model system with potential for the study of plant reproduction. *Plant Cell* **5**: 1483–1488.

Elliott RC, Betzner AS, Huttner E, Oakes MP, Tucker W, Gerentes D, Perez P, Smyth DR. 1996. AINTEGUMENTA, an APETALA2-like gene of Arabidopsis with pleiotropic roles in ovule development and floral organ growth. *Plant Cell* **8**: 155–168.

Frank MH, Scanlon MJ. 2015. Cell-specific transcriptomic analyses of three-dimensional shoot development in the moss *Physcomitrella patens*. *The Plant Journal* **83**: 743–751.

Galinha C, Hofhuis H, Luijten M, Willemsen V, Blilou I, Heidstra R, Scheres B. 2007. PLETHORA proteins as dose-dependent master regulators of Arabidopsis root development. *Nature* **449**: 1053–1057.

Graham LE, Cook ME, Busse JS. 2000. The origin of plants: body plan changes contributing to a major evolutionary radiation. *Proceedings of the National Academy of Sciences, USA* **97**: 4535–4540.

Harrison CJ, Roeder AH, Meyerowitz EM, Langdale JA. 2009. Local cues and asymmetric cell divisions underpin body plan transitions in the moss *Physcomitrella patens*. *Current Biology* **19**: 461–471.

Kofuji R, Hasebe M. 2014. Eight types of stem cells in the life cycle of the moss *Physcomitrella patens*. *Current Opinion in Plant Biology* **17**: 13–21.

Kosetsu K, Murata T, Yamada M, Nishina M, Boruc J, Hasebe M, Van Damme D, Goshima G. 2017. Cytoplasmic MTOCs control spindle orientation for asymmetric cell division in plants. *Proceedings of the National Academy of Sciences, USA* **114**: E8847–E8854.

Kerstens M, Strauss S, Smith R, Willemsen V. 2019. From stained plant tissues to quantitative cell segmentation analysis with MorphoGraphX. *Methods Molecular Biology*. doi: 10.1007/978-1-0716-0342-0.

Moody LA, Kelly S, Rabbinowitsch E, Langdale JA. 2018. Genetic regulation of the 2D to 3D growth transition in the moss *Physcomitrella patens*. *Current Biology* **28**: 473–478.

Nishiyama T, Hiwatashi Y, Sakakibara K, Kato M, Hasebe M. 2000. Tagged mutagenesis and gene-trap in the moss, *Physcomitrella patens* by shuttle mutagenesis. *DNA Research* **7**: 9–17.

Perroud PF, Demko V, Johansen W, Wilson RC, Olsen OA, Quatrano RS. 2014. Defective Kernel 1 (DEK1) is required for three-dimensional growth in *Physcomitrella patens*. *New Phytologist* **203**: 794–804.

Pillitteri LJ, Guo X, Dong J. 2016. Asymmetric cell division in plants: mechanisms of symmetry breaking and cell fate determination. *Cellular and Molecular Life Sciences* **73**: 4213–4229.

Polyn S, Willems A, De Veylder L. 2015. Cell cycle entry, maintenance, and exit during plant development. *Current Opinion in Plant Biology* **23**: 1–7.

Prigge MJ, Bezanilla M. 2010. Evolutionary crossroads in developmental biology: *Physcomitrella patens*. *Development* **137**: 3535–3543.

de Reuille PB, Routier-Kierzkowska A-L, Kierzkowski D, Bassel GW, Schüpbach T, Tauriello G, Bajpai N, Strauss S, Weber A, Kiss A. 2015. MorphoGraphX: a platform for quantifying morphogenesis in 4D. *eLife* **4**: e05864.

Scheres B, Wolkenfelt H, Willemsen V, Terlouw M, Lawson E, Dean C, Weisbeek P. 1994. Embryonic origin of the Arabidopsis primary root and root meristem initials. *Development* **120**: 2475–2487.

Schindelin J, Arganda-Carreras I, Frise E, Kaynig V, Longair M, Pietzsch T, Preibisch S, Rueden C, Saalfeld S, Schmid B. 2012. Fiji: an open-source platform for biological-image analysis. *Nature Methods* **9**: 676.

van Gisbergen PA, Wu S-Z, Chang M, Pattavina KA, Bartlett ME, Bezanilla M. 2018. An ancient Sec10–formin fusion provides insights into actin-mediated regulation of exocytosis. *The Journal of Cell Biology* **217**: 945–957.

Whitewoods CD, Cammarata J, Nemec Venza Z, Sang S, Crook AD, Aoyama T, Wang XY, Waller M, Kamisugi Y, Cuming AC *et al.* 2018. *CLAVATA* was a genetic novelty for the morphological innovation of 3D growth in land plants. *Current Biology* **28**: 2365–2376.

Yamada M, Miki T, Goshima G. 2016. Imaging mitosis in the moss *Physcomitrella patens*. In: Chang P, Ohi R, eds. *The mitotic spindle. Methods in molecular biology, vol. 1413*. New York, NY, USA: Humana Press, 263–282.

Yoshida S, Barbier de Reuille P, Lane B, Bassel GW, Prusinkiewicz P, Smith RS, Weijers D. 2014. Genetic control of plant development by overriding a geometric division rule. *Developmental Cell* **29**: 75–87.

Supporting Information

Additional Supporting Information may be found online in the Supporting Information section at the end of the article.

Fig. S1 Swelling gametophore initial cells develop into early gametophores.

Fig. S2 The longitudinal cell lengths in gametophore or branch initial cells for MGX analysis do not show differences.

Fig. S3 The width of branch initial cells in Δ*dek1* is similar to the width of wild-type branch initial cells.

Fig. S4 Quantification of the NLS4-GFP-GUS intensity in gametophore and branch initials relative to their parental cells.

Video S1 Time-lapse imaging shows four examples of the gametophore development from swelling to early gametophores with multiple divisions.

Video S2 Time-lapse imaging reveals the rate of NLS4-GFP-GUS fluorescence decay during swelling of a gametophore initial cell.

Please note: Wiley Blackwell are not responsible for the content or functionality of any Supporting Information supplied by the authors. Any queries (other than missing material) should be directed to the *New Phytologist* Central Office.